Electronic Supplementary Material (ESI) for Nanoscale.


## Supporting Information

# Anti-KIT DNA Aptamer-conjugated Porous Silicon Nanoparticles for the Targeted Detection of Gastrointestinal Stromal Tumors

Sanahan Vijayakumar[1], Seyedmehdi H. Nasr[2], Jacob E. Davis[3,4], Edward Wang[1], Jonathan M. Zuidema[2,5], Yi-Sheng Lu[1], Yu-Hwa Lo[1,6], Jason K. Sicklick[3,4,7], Michael J. Sailor*[1,2], and Partha Ray*[3,4]

[1]Materials Science and Engineering Program, University of California, San Diego, La Jolla, California, 92093, United States

[2]Department of Chemistry & Biochemistry, University of California, San Diego, La Jolla, California, 92093, United States

[3]Department of Surgery, Division of Surgical Oncology, University of California, San Diego, San Diego, California, 92093, United States

[4]Moores Cancer Center, University of California, San Diego, La Jolla, California, 92093, United States

[5]Department of Neurosciences, University of California, San Diego, San Diego, California, 92093, United States

[6]Department of Electrical & Computer Engineering, University of California, San Diego, La Jolla, California, 92093, United States

[7]Department of Pharmacology, University of California, San Diego, San Diego, California, 92093, United States

*Corresponding Author

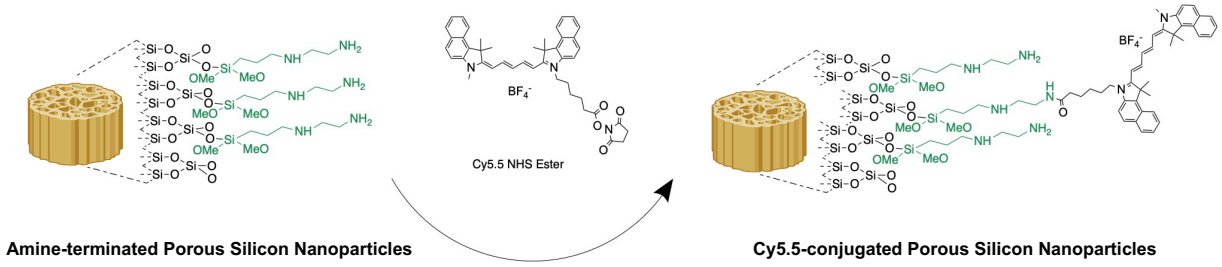


Figure S1. Preparation of dye-conjugated pSiNPs. Schematic illustration of the attachment of Cy5.5 NHS Ester to amine terminated pSiNPs (pSiNP-$NH_2$) to form pSiNP-$NH_2$-Cy5.5 particles.

Table S1. Characteristics of pSiNP constructs for pore structure and internal surface area as calculated from cryogenic nitrogen adsorption isotherms. [a]Values determined using BET (Brunnauer–Emmett–Teller) analysis of the adsorption isotherms. [b]Values determined using BJH (Barret–Joyner–Halenda) analysis of the adsorption/desorption isotherms (mean value ± SD, n = 3).

| **$N_2$ Adsorption/Desorption Isotherms** | | | |
|---|---|---|---|
| | **pSiNP** | **pSiNP-$NH_2$** | **pSiNP-$NH_2$-PEG-KIT** |
| **Surface Area ($m^2$/g)[a]** | 333.43 ± 14.71 | 119.25 ± 22.76 | 102.04 ± 8,44 |
| **Pore Volume ($cm^3$/g)[b]** | 1.38 ± 0.08 | 0.46 ± 0.03 | 0.42 ± 0.07 |
| **Pore Size (nm)[b]** | 14.75 ± 0.13 | 14.13 ± 0.05 | 13.44 ± 0.10 |

Table S2. Size & Surface Charge of pSiNP Constructs as assessed through Dynamic Light Scattering (mean value ± SD, n = 3).

| **Hydrodynamic Size & Surface Charge** | | | | | |
|---|---|---|---|---|---|
| | **pSiNP** | **pSiNP-$NH_2$** | **pSiNP-$NH_2$-Cy5.5** | **pSiNP-$NH_2$-Cy5.5-PEG** | **pSiNP-$NH_2$-Cy5.5-PEG-KIT** |
| **Z-Avg. Size (nm)** | 156.3 ± 6.5 | 168.4 ± 1.4 | 186.2 ± 8.6 | 228.2 ± 3.9 | 237.8 ± 1.1 |
| **ζ-Potential (mV)** | -27.53 ± 1.63 | 14.22 ± 1.07 | 3.17 ± 0.67 | 6.65 ± 1.23 | 2.33 ±1.02 |

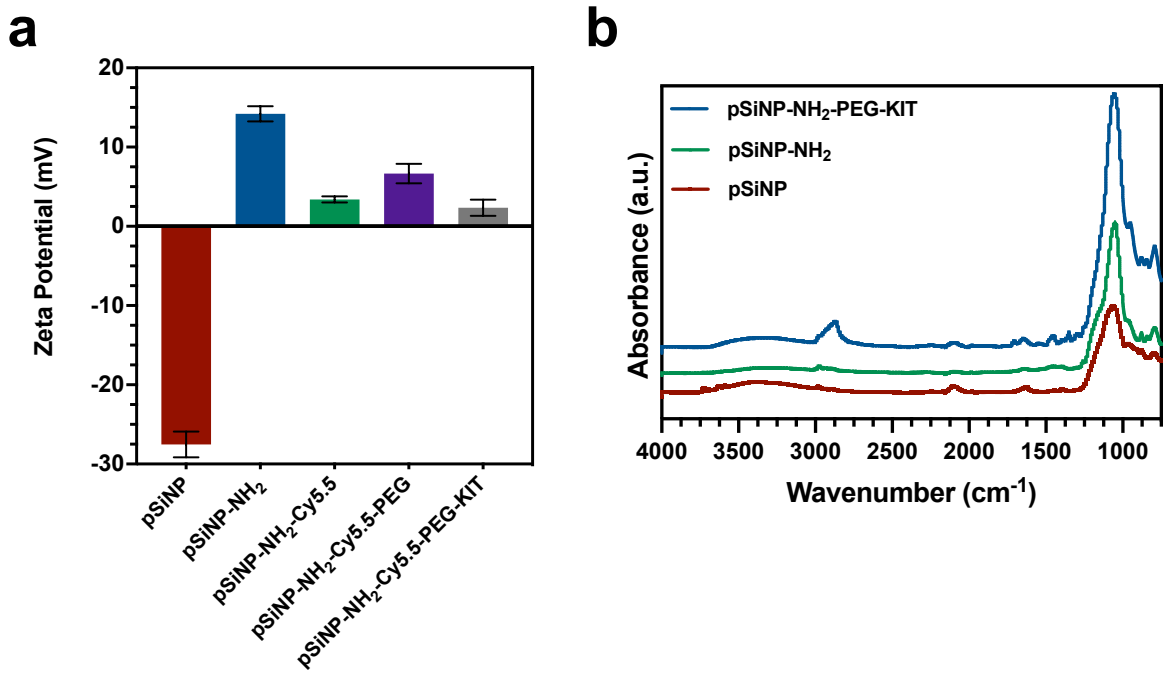


Figure S2. Characterization of pSiNP constructs. (a) Zeta potential measurements of as-prepared pSiNPs, amine-functionalized pSiNPs (pSiNP-$NH_2$), dye-loaded amine-functionalized pSiNPs (pSiNP-$NH_2$-Dye), PEGylated pSiNPs (pSiNP-$NH_2$-Dye-PEG) and KIT-aptamer conjugated, dye-loaded PEGylated pSiNPs (pSiNP-$NH_2$-Dye-PEG-KIT) respectively (mean value ± SD, n = 3). Error bars represent standard deviation of three independently prepared samples. (b) Fourier Transform Infrared Spectroscopy (FTIR) spectra of pSiNPs functionalized with cyclic-silanes and PEG.

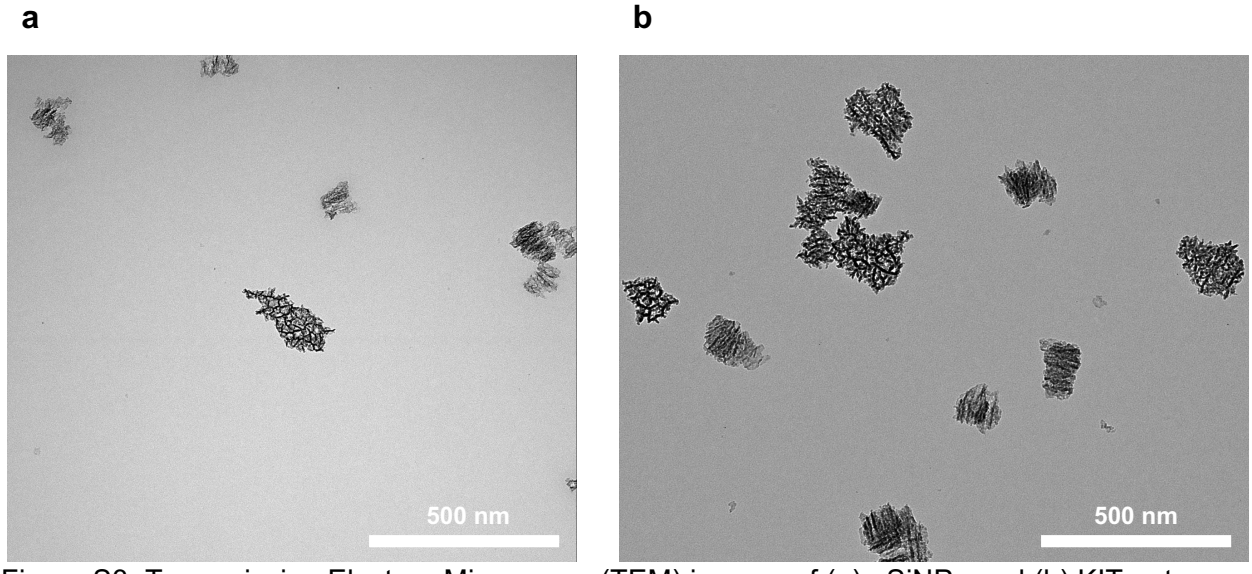


Figure S3. Transmission Electron Microscopy (TEM) images of (a) pSiNPs and (b) KIT aptamer-conjugated, Cy5.5-loaded, PEGylated particles (pSiNP-$NH_2$-Cy5.5-PEG-KIT) (scale bar = 500 nm).

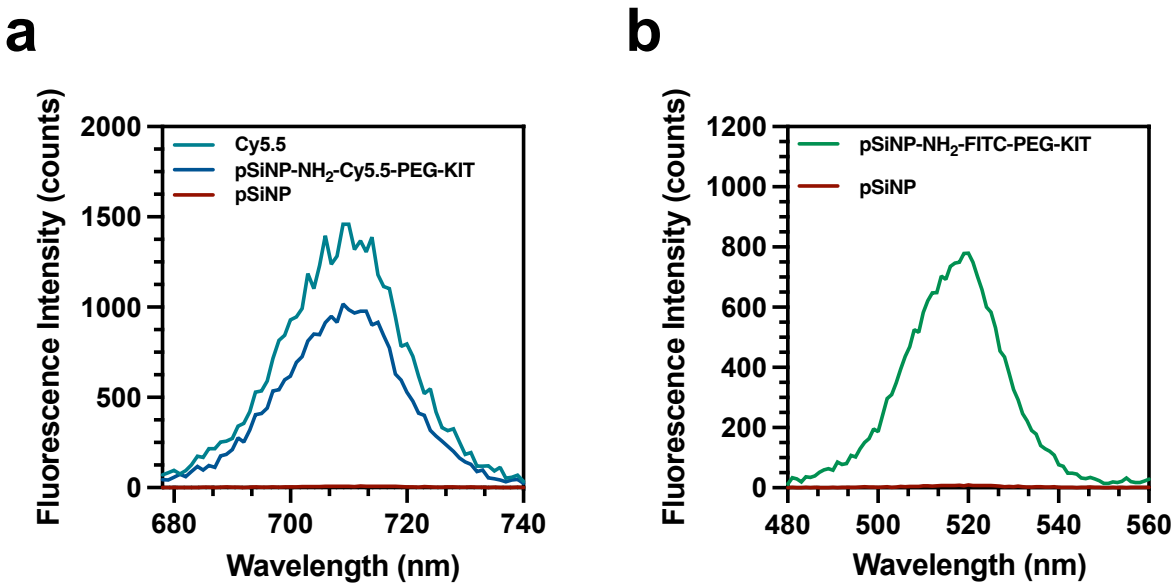


Figure S4. Characterization of dye-conjugated pSiNPs. (a) Fluorescence measurement of Cy5.5 loaded pSiNPs. (b) Fluorescence measurement of FITC loaded pSiNPs.

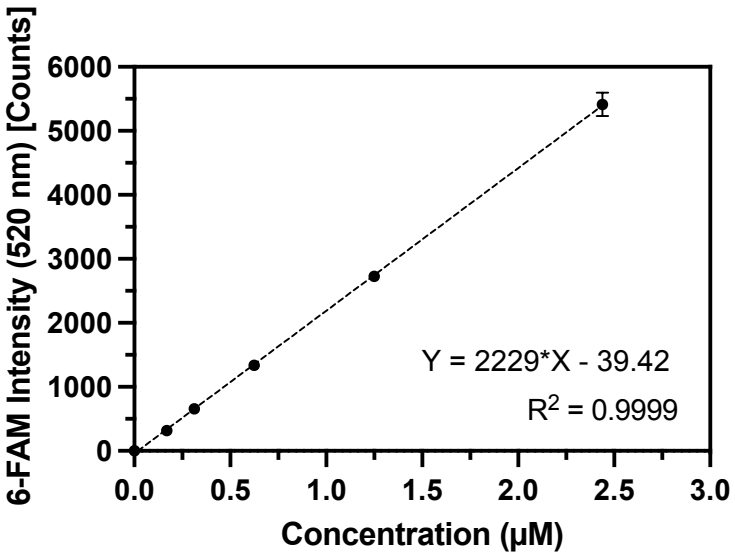


Figure S5. Standard curve of 6-FAM-conjugated KIT-aptamer (mean value ± SD, n = 3). The aptamer concentration is correlated to the 6-FAM intensity at 520 nm and is used to quantify the concentration of aptamers bound to the pSiNPs.

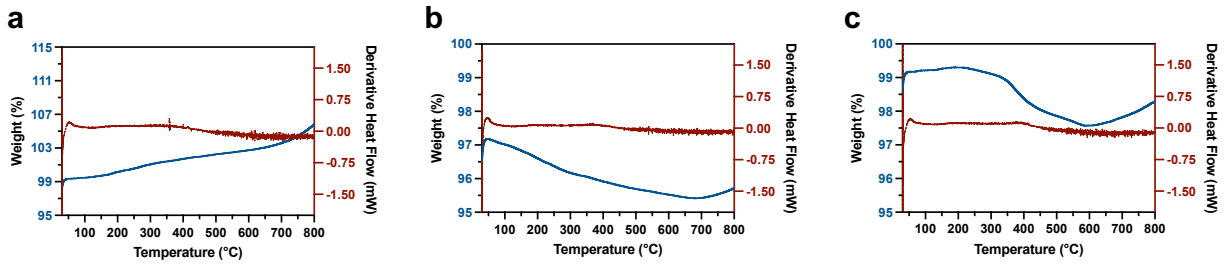


Figure S6. Thermogravimetric analysis (TGA) measurements of (a) pSiNP, (b) pSiNP-$NH_2$ and (c) pSiNP-$NH_2$-PEG. The derivative heat flow indicates phase changes of the silane-coated and PEGylated particles while the weight (%) curve provides an estimate of the amount of conjugated material is available in a given amount of nanoparticles. The measurements indicated a weight percent loss of 1.98% (wt.) for the cyclic azasilane reagent which overlapped with a melting temperature from 71-73°C[1], as seen in (b) for the weight percent change. For (c), the determined weight percent loss for the MAL-PEG-SVA overcoat was 0.17% (wt.), determined by the melting point region from 182-287°C for the PEG[2]. These calculated values were used to determine levels of toxicity for the synthetic reagents for both *in vitro* and *in vivo* experiments.

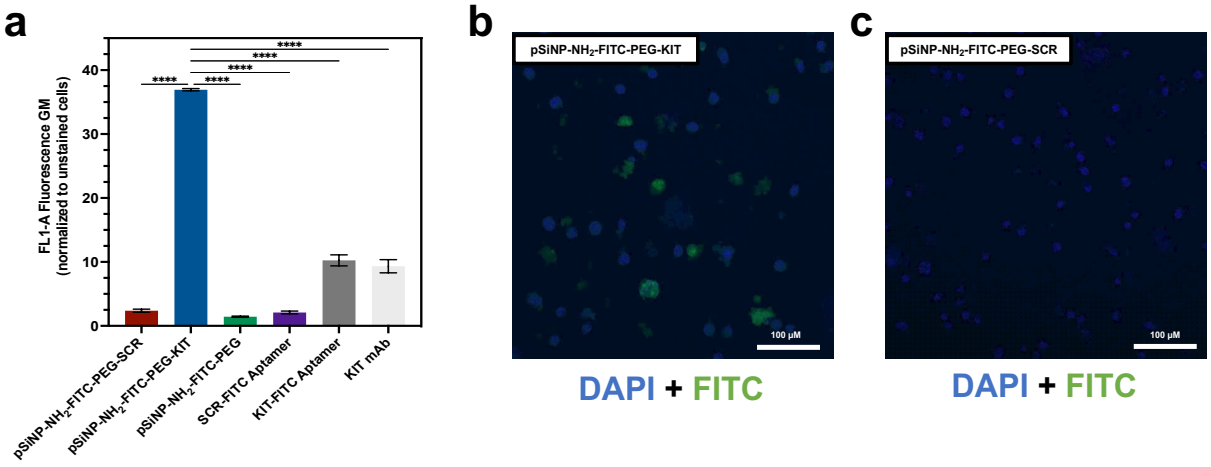


Figure S7. Investigation of cellular targeting of aptamer-conjugated pSiNPs in a model HMC-1.2 cancer cell line. (a) Flow cytometry data evaluating the efficacy of the aptamer-conjugated pSiNP group to localize to GIST-T1 cells, quantified as a normalized FL1-A Fluorescence GM attached to the particles and aptamers, versus free KIT aptamer and scramble controls (mean value ± SD, n = 3, *p < 0.0001). Confocal microscopy images of HMC-1.2 cells incubated with (b) FITC-labelled, KIT-aptamer conjugated pSiNPs and (c) FITC-labelled, Scramble-aptamer control conjugated pSiNPs. Both images are merged laser lines for DAPI and FITC (scale bar = 100 µm).

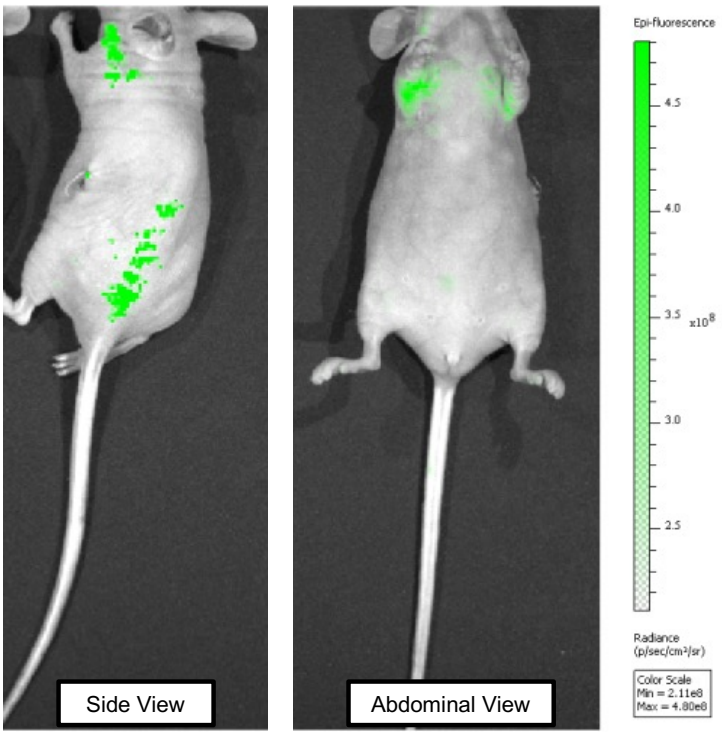


Figure S8. Temporal IVIS images of 5-week-old tumor burden GIST-T1 mice. GFP signals from the GIST-T1 tumors are visible in green for both the side and abdominal view of the mouse. There is a visible GFP signal within the thorax region of the mice, indicative of the lymph nodes. It is known that cancers would migrate to this region as part of the host's auto-immune response.[3]

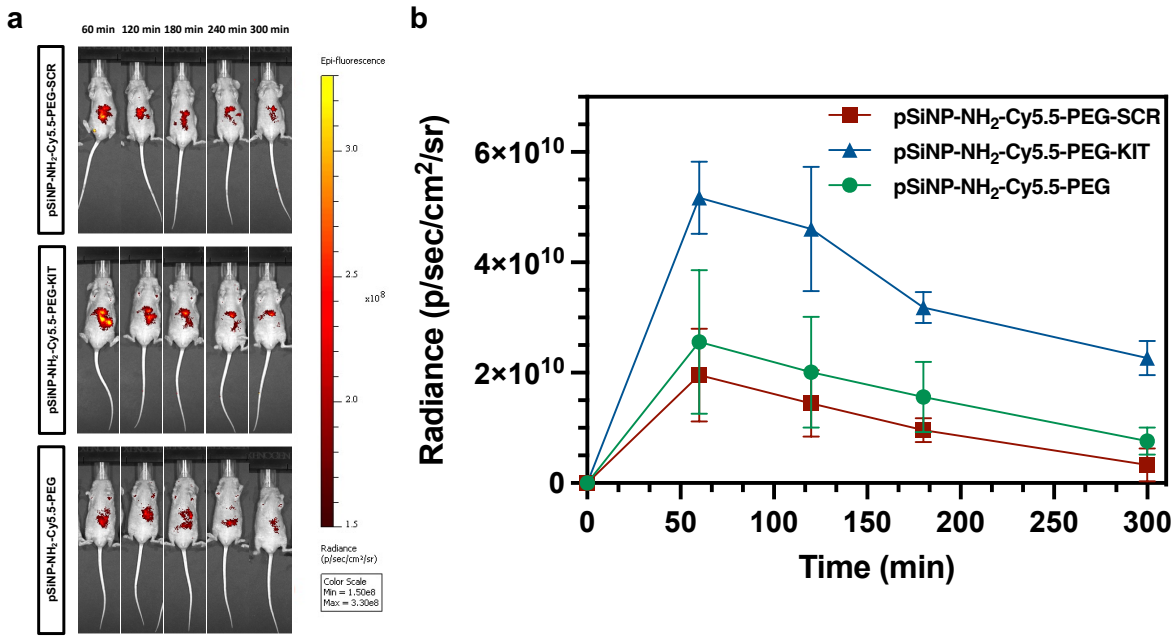


Figure S9. Temporal *in vivo* IVIS imaging. (a) Temporal IVIS images of 5-week-old GIST-T1 mice injected with pSiNP constructs tail-vein. Cy5.5 signals, of the pSiNP constructs were isolated from abdomen regions after every hour for 5 hours. Isolated Cy5.5 signals from abdomen regions measuring (b) total radiance (p/sec/cm2/sr) for measured signals (mean value ± SD, n = 3).

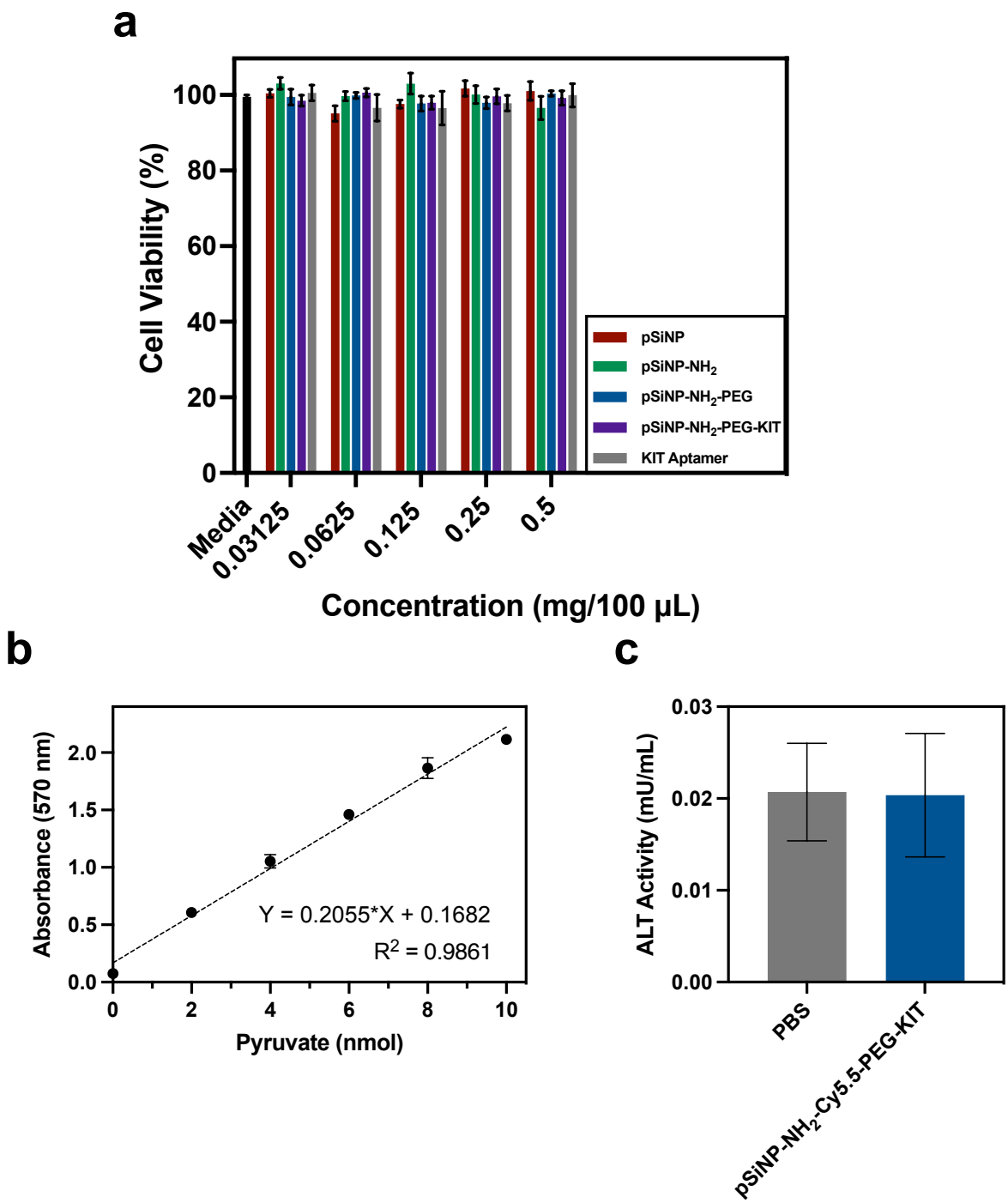


Figure S10. Biosafety Analysis of pSiNP constructs. (a) Viability of RAW 264.7 macrophage cells incubated with various concentrations of pSiNP constructs for 48 hours. Error bars indicate SD (mean value ± SD, n = 3, $p < 0.05$). Serum ALT assay to measure liver toxicity due to pSiNP constructs. (b) Standard curve to assess Pyruvate activity and (c) ALT activity of serum collected from pSiNP-$NH_2$-Cy5.5-PEG-KIT and PBS injected mice (mean value ± SD, n = 3). Aptamer-pSiNP constructs showed no significant effects on ALT value when compared to PBS controls.

Table S3. Histopathological analysis of harvested organs, liver, spleen, and kidneys of pSiNP injected mice compared to PBS controls. Analysis was completed by by Dr. Valeria Estrada, MD (UCSD Moores Cancer Center).

| Histopathological Findings | |
|---|---|
| | **Comments** |
| Mouse 1 (PBS) - Kidney | No Pathological Findings |
| Mouse 1 (PBS) - Spleen | No Pathological Findings |
| Mouse 1 (PBS) - Liver | No Pathological Findings |
| Mouse 3 (pSiNP) - Kidney | No Pathological Findings |
| Mouse 3 (pSiNP) - Spleen | No Pathological Findings |
| Mouse 3 (pSiNP) - Liver | No Pathological Findings |
| Mouse 4 (pSiNP-KIT) - Kidney | No Pathological Findings |
| Mouse 4 (pSiNP-KIT) - Spleen | No Pathological Findings |
| Mouse 4 (pSiNP-KIT) - Liver | No Pathological Findings |

## References


1. D. Kim, J. M. Zuidema, J. Kang, Y. Pan, L. Wu, D. Warther, B. Arkles and M. J. Sailor, *Journal of the American Chemical Society*, 2016, **138**, 15106-15109.
2. S. Aksakal, R. Aksakal and C. R. Becer, 2021, DOI: https://doi.org/10.1002/9783527823819.ch7, 235-263.
3. H. Zhou, P.-j. Lei and T. P. Padera, *Journal*, 2021, **10**.